[Li−Si−O]-MFI: A New Microporous Lithosilicate with the MFI Topology

So-Hyun Park,[†,||] Haiming Liu,[‡] Martin Kleinsorge,[†,‡] Clare P. Grey,[‡] Brian H. Toby,[§] and John B. Parise*[,†,‡]

Departments of Geosciences and Chemistry, State University of New York at Stony Brook, New York 11790-2100

Received January 24, 2004. Revised Manuscript Received March 17, 2004

We report the synthesis and structure solution of [Li−Si−O]-MFI (a = 19.793(4) Å, b = 19.766(4) Å, c = 13.266(3) Å, space group $P2_12_12_1$), a framework zeolite related to ZSM-5 (silicalite) with a Li/Si ratio of 4:92. Single-crystal synchrotron X-ray diffraction data, ^{29}Si NMR, and infrared spectroscopy indicate that the Li is randomly distributed over the framework sites. In addition, Li occupies ordered positions on extraframework sites that are occluded in voids outlined by the double five- or six-membered rings. The strong interaction between the extraframework Li cations and the negatively charged framework may be responsible for the distortion of the lattice from *Pnma*, the usual symmetry associated with as-synthesized members of the MFI-family, to its subgroup symmetry $P2_12_12_1$. Variable-temperature ^{7}Li and ^{1}H MAS NMR experiments show that the extraframework Li cations are not directly accessible to gas molecules, but that the protons formed on calcination are accessible.

Introduction

The synthesis of new microporous frameworks[1] and the manipulation of known zeolite structural types are important first steps in expanding the catalog of selective catalysts and materials for separation processes.[2,3] We recently reported the synthesis and structure determination of a series of new framework materials structurally related to the aluminosilicate zeolites, but containing substantial incorporation of Li in the framework.[4,5] These materials contain structural moieties, such as the (Li,Si)-spiro-3,5 and (Li,Si)-spiro-3 secondary building units (SBU) with strain-free three-membered rings that differ from those usually encountered in silicate chemistry. This, in turn, leads to novel topologies where the lithium ions are segregated into separate building units. In the structure of $Cs_{14}Li_{24}[Li_{18}Si_{72}O_{172}]\cdot 14H_2O$ (RUB-29), the Li cations are disordered over sites that are closely spaced (∼2.5 Å). This is stable presumably because of the comparatively low repulsion between neighboring monovalent Li^+ cations and the partial occupancy of the closely spaced sites.[6] This proximity of sites in edge-sharing [LiO_4]-tetrahedra and layered SBUs favors high lithium-ion mobility.[7]

The catalytic and sorption properties of zeolites may be dramatically varied by changing the Si^{4+}/Al^{3+} ratio of the aluminosilicate framework. Although other replacements for Si^{4+} are known, introduction of a monovalent cation into the framework leads to the highest possible local charge imbalance per substitution. Our discovery of these novel microporous lithosilicates suggests that *known* high-silica materials, and possibly aluminosilicates, may also accommodate significant amounts of lithium in their frameworks. Substitution of framework Si^{4+} ions by Li^+ ions requires three times more charge-balancing M^+ extraframework cations, in comparison to Al^{3+} substitution. This added variability in the charge distributions within the channel systems of high-silica zeolites might lead to new ion-exchange, and acid and gas sorption properties. Our reports of an Li-substituted zincosilicate ($Cs_{12}Li_{13}[Li_3Zn_8Si_{37}O_{96}]\cdot 4H_2O$), with a structure related to analcime (ANA), is an example of the success of the strategy outlined above.[8] This new material contains partially ordered

* To whom correspondence should be addressed. E-mail: jparise@notes.cc.sunysb.edu. Phone: +1-631-632-8196. Fax: +1-631-632-8140.
† Department of Geosciences.
‡ Center for Environmental Molecular Sciences and Chemistry Department.
§ NIST Center for Neutron Research, National Institute of Standards and Technology, Gaithersburg, MD 20899-8562.
|| Current address: Department für Geo- und Umweltwissenschaften, Sektion Kristallographie, Ludwig-Maximilians-Universität München, 80333 München, Germany. E-mail: sohyun.park@physik.uni-muenchen.de.

(1) Meier, W. M., Olson, D. H., Baerlocher, Ch., Eds. *Atlas of Zeolite Structure Types*, 4th ed.; Structure Commission of the International Zeolite Association, Elsevier: New York, 1996.
(2) Flanigen, E. M. *Proceedings of the 5th International Conference on Zeolites*; Rees, L. V. C., Ed.; Heyden and Son Ltd.: Chichester, 1980; pp 760−780.
(3) Flanigen, E. M. In *Textbook of Introduction to Zeolite Science and Practice*; van Bekkum, H., Flanigen, E. M., Jansen, J. C., Eds.; Elsevier: Amsterdam, 1991; pp 13−34.
(4) Park, S.−H.; Daniels, P.; Gies, H. *Microporous Mesoporous Mater.* **2000**, *37*, 129−143.
(5) Park, S.-H.; Parise, J. B.; Gies, H.; Liu, H.; Grey, C. P.; Toby, B. H. *J. Am. Chem. Soc.* **2000**, *122*, 11023−11024.
(6) Park, S.-H.; Parise, J. B.; Gies, H. In *Zeolites and Mesoporous Materials at the Dawn of the 21st Century: Proceedings of the 13th International Zeolite Conference*; *Studies in Surface Science and Catalysis*, vol. 135, [CD-ROM] Paper 09-O-05; Galarneau, A., Di Renzo, F., Fajula, F., Vedrine, J., Eds.; Elsevier: New York, 2001.
(7) Franke, M. E.; Rodriguez-Gonzales, L.; Simon, U.; Park, S.-H. In *Book of Abstracts, Proceedings of 16th German Zeolite Conference in Dresden*, March 2004 German Zeolite Association (Fachsektion Zeolithe der Dechema), (http://cpchol.chm.tu-dresden.de/zeolith.2004/)

10.1021/cm049861n CCC: $27.50
Published on Web 05/26/2004

tetrahedral framework (T) sites occupied by Li, Zn, and Si atoms. The material shows the highest ratio among ANA family members of nonframework cations (M) to substituting T atoms, i.e., with M/T = 2.3:1. However, the distorted channel system of this new ANA material, with a narrow pore opening of 1.6 × 4.2 Å^2, makes its use in gas separation or catalytic processes unlikely.

We chose silicalite, the pure silica form of the aluminosilicate ZSM-5 which adopts the MFI topology,[9] as a target system for Li-framework substitution into a structure type with increased porosity. This thermally stable molecular sieve contains two different channel systems: straight- and sinusoidal-channels bounded by 10-membered rings of corner-connected SiO_4-tetrahedra with a pore opening size of 5.3 × 5.6 Å^2 and 5.1 × 5.5 Å^2, respectively[1]. Because of this unique channel structure, MFI and its variants based on the substitution of Si^{4+} by cations such as Al, As, B, Fe, Ga, and Ti, are used for a range of catalytic applications.[10−12] Here we report the first example of substantial Li substitution into the ZSM-5 framework to form the new ZSM-5 family member [Li−Si−O]-MFI. This new material may be representative of a more general capability of Li to replace Si in other known high-silica microporous materials.

Experimental Section

Synthesis of Microporous Materials. A typical synthesis for [Li−Si−O]-MFI is as follows. A 21.79-mL aliquot of tetrapropylammonium hydroxide (TPAOH, 40% aqueous solution, Alfa) and 0.90 g of lithium hydroxide monohydrate (LiOH·H_2O, Alfa) were added to 20 mL of distilled water with stirring to give a homogeneous basic solution. Tetramethoxysilane (6.35 mL TMOS, >98%, Alfa) was added (as a silicon source) to the solutions while vigorously stirring (1 drop per 10 s). After aging for 2−3 h at room temperature, the mixture was charged into 22-mL Teflon-lined stainless steel autoclaves (Parr) and then allowed to react under static hydrothermal conditions by heating at 175 °C for 7 days. The gel has a molar composition of 0.5:1:1:44 = $LiOH/SiO_2/TPAOH/H_2O$.

The synthesis product contained crystalline solid phases dispersed in a clear solution. As-synthesized samples were prepared by filtering and washing with distilled water and ethanol several times and then drying at room-temperature overnight. Calcined samples were obtained by removing organic template molecules from the as-synthesized material by heating at 823 K in air for 7 days.

To compare the infrared spectra of [Li−Si−O]-MFI to those of the Li-free sample and to those with Li at extraframework positions alone, pure silica ZSM-5 (silicalite) and Li-exchanged aluminosilicate ZSM-5 were prepared. Silicalite was synthesized from a starting mixture with a molar composition of 1:0.5:44 = SiO_2/TPAOH/H_2O under hydrothermal conditions at 180 °C for 7 days. A sample designated Li−ZSM-5(Al) with composition $Li_{3.3}[Al_{3.3}Si_{93.7}O_{192}]\cdot xH_2O$ was provided by Professor David H. Olson at the Department of Chemical Engineering, University of Pennsylvania. It was prepared as follows. H−ZSM-5 (Si/Al = 29) (5 g) was exchanged at 25 °C with 250 mL of 0.5 N $LiNO_3$ (Fisher certified). The pH was quickly adjusted to 8.7 by dropwise addition of 1.0 N LiOH (Fisher purified) and the mixture was left for an hour. The product was washed on filter paper with 150 mL of deionized water.

Characterization. The microporous materials produced were examined by X-ray powder diffraction (XPD) on a Scintag diffractometer with Cu Kα radiation at 25 mA and 40 kV in the 2θ region of 5 to 50° with a scan speed of 2° min^{-1}. To increase signal-to-noise discrimination the sample was placed on a plate of single-crystal quartz.

The Si, Li, C, and N contents of a powdered sample of as-synthesized [Li−Si−O]-MFI were determined by Galbraith Laboratories, Inc., Knoxville, TN.

Magic angle spinning nuclear magnetic resonance (MAS NMR) experiments were performed with a double-tuned Chemagnetics 5-mm probe on a CMX-360 spectrometer. ^{29}Si MAS NMR spectra on an as-synthesized [Li−Si−O]-MFI sample were acquired at an operating frequency of 71.52 MHz and a spinning speed of 5.0 kHz, with $\pi/2$ pulses of 4 μs and recycle delays of 120 s. Proton decoupling was applied to remove the ^{29}Si−^{1}H heteronuclear coupling. ^{29}Si spectra were referenced to TMS at 0 ppm. Spectra for ^{7}Li were accumulated at a frequency of 139.92 MHz with a dehydrated, calcined [Li−Si−O]-MFI sample loaded with 100 Torr of O_2 in a sealed Pyrex capsule. The ^{7}Li spectra were acquired with a spinning speed of 10.0 kHz, with $\pi/4$ pulses of 2 μs and recycle delays of 20 s, and referenced to 1 M LiCl at 0 ppm. ^{1}H MAS NMR spectra of another sample of dehydrated [Li−Si−O]-MFI were obtained at a frequency of 360.0 MHz with a spinning speed of 4.0 kHz. $\pi/2$ excitation pulses of 4 μs and recycle delays of 2 s were used, and the spectra were referenced to $CHCl_3$ at 7.24 ppm.

Silicalite and Li−ZSM-5(Al) should contain no Li−O−Si linkages in their framework structures whereas [Li−Si−O]-MFI should, if Li substitutes for Si. To observe any differences that might exist in the IR spectra of these three different MFI family members, samples were studied in the wavenumber region of 4000−400 cm^{-1} on a Nicolet Nexus 670 FT-IR spectrometer using KBr as a window material. An additional IR spectrum of a dehydrated sample of calcined [Li−Si−O]-MFI was obtained under dried nitrogen atmosphere on a Nicolet Magna 750 IR spectrometer.

Data collection for the crystallographic experiments was conducted at beamline 13-ID of the GeoSoilEnviro Consortium for Advanced Radiation Science (GSE-CARS) of the Advanced Photon Source (APS) of Argonne National Laboratory. A twinned crystal of [Li−Si−O]-MFI (10 × 5 × 2 μm^3) was used to collect intensity data on a Bruker area detector (charge coupled device) with a graphite monochromator (λ = 0.689(3) Å). The data set consisted of 46004 reflections harvested from 1530 frames collected in the $\theta/2\theta$ scan mode (θ_{max} = 31°) at a counting time of 2 s per frame. Of these, 6605 symmetrically nonequivalent reflections were obtained in the selected Laue group *mmm* (R_{ini} = 0.06). The reflections were corrected for absorption by using the program SADABS distributed by Bruker Analytical.[13] Using 5537 observations with [$|F_o| > 4\sigma(|F_o|)$], the crystal structure was determined by direct methods, Fourier calculation, and by Fourier difference synthesis with program package SHELXTL from Bruker.[13]

Structural Analysis. Single-crystal structure analysis using the microcrystal of [Li−Si−O]-MFI revealed it consists of two twin individuals related by a rotation 90° about the shared *c*-axis. The applied twin matrix is (0 −1 0/1 0 0/0 0 1). Systematic extinctions uniquely identify the space group as $P2_12_12_1$ and lattice parameters are a = 19.793(4) Å, b = 19.766(4) Å, c = 13.266(3) Å. This space group for the as-synthesized [Li−Si−O]-MFI material differs from the usual symmetry associated with as-synthesized members of the MFI-family (*Pnma*).[14]

(8) Park, S.-H.; Gies, H.; Toby, B. H.; Parise, J. B. *Chem. Mater.* **2002**, *14*, 3187−3196.

(9) Flanigen, E. M.; Bennett, J. M.; Grose, R. W.; Cohen, J. P.; Patton, R. L.; Kirchner, R. M.; Smith, J. V. *Nature* **1978**, *271*, 512−516.

(10) Materials related to the MFI structure are summarized in the database of *Zeolite Structures by International Zeolite Association* (http://www.zeolites.ethz.ch/zeolites/..).

(11) Gabelica, Z.; Valange, S. *Microporous Mesoporous Mater.* **1999**, *30* (1), 57−66.

(12) Tuan, V. A.; Falconer, J. L.; Noble, R. D. *Microporous Mesoporous Mater.* **2000**, *41* (1−3), 269−280.

(13) Data collection, reduction, and analysis were conducted using program packages of Bruker Analytical X-ray Systems, SMART (version 5.0, 1997), SAINT (version 4, 1994−1996) including SADABS, and SHELXTL (version 5.10, 1998) for Windows NT, respectively.

(14) van Koningsveld, H.; van Bakkum, H.; Jansen, J. C. *Acta Crystallogr.* **1987**, *B43*, 127−132.

Table 1. Structural Parameters for [Li−Si−O]-MFI ($TPA_4Li_8[Li_4Si_{92}O_{192}]$) from Synchrotron Single-Crystal Diffraction Data[a]

site	M^b	x	y	z	occupancy	$U_{iso}{}^c$	site	M^b	x	y	z	occupancy	$U_{iso}{}^c$
T1	4	0.4228(2)	0.0572(2)	0.9135(2)	1 [0.96(1)][d]	0.018(1)	O19	4	0.1946(5)	0.9984(4)	0.8474(6)	1	0.038(2)
T2	4	0.3075(2)	0.0283(2)	0.0598(2)	1 [0.95(1)][d]	0.019(1)	O20	4	0.1973(5)	0.8718(5)	0.8332(7)	1	0.047(2)
T3	4	0.2788(2)	0.0613(2)	0.2823(2)	1 [0.97(1)][d]	0.016(1)	O21	4	0.9959(5)	0.0472(6)	0.0459(7)	1	0.041(3)
T4	4	0.1223(2)	0.0627(2)	0.2778(2)	1 [0.96(1)][d]	0.012(1)	O22	4	0.9964(5)	0.8490(5)	0.0436(7)	1	0.042(3)
T5	4	0.0712(2)	0.0277(1)	0.0667(2)	1 [0.98(1)][d]	0.013(1)	O23	4	0.4216(3)	0.7499(6)	0.8980(4)	1	0.036(1)
T6	4	0.1865(2)	0.0591(2)	0.9229(2)	1 [0.96(1)][d]	0.017(1)	O24	4	0.1873(3)	0.7498(5)	0.8967(4)	1	0.039(1)
T7	4	0.4230(2)	0.8272(2)	0.9232(2)	1 [0.94(1)][d]	0.016(1)	O25	4	0.2858(3)	0.7516(6)	0.3061(4)	1	0.035(1)
T8	4	0.3071(2)	0.8693(2)	0.0633(2)	1 [0.96(1)][d]	0.019(1)	O26	4	0.1090(3)	0.7534(5)	0.3104(4)	1	0.024(1)
T9	4	0.2759(2)	0.8276(1)	0.2812(2)	1 [0.95(1)][d]	0.017(1)	O27	4	0.6268(5)	0.9400(5)	0.4960(6)	1	0.041(2)
T10	4	0.1197(2)	0.8278(2)	0.2808(2)	1 [0.94(1)][d]	0.022(1)	O28	4	0.6925(4)	0.9393(4)	0.3283(5)	1	0.027(2)
T11	4	0.0705(2)	0.8703(2)	0.0686(2)	1 [0.97(1)][d]	0.019(1)	O29	4	0.7995(5)	0.9431(5)	0.2218(6)	1	0.050(2)
T12	4	0.1871(2)	0.8264(2)	0.9307(2)	1 [0.94(1)][d]	0.022(1)	O30	4	0.9059(4)	0.9395(5)	0.3315(6)	1	0.042(2)
T13	4	0.5774(2)	0.9429(2)	0.5843(2)	1 [0.96(1)][d]	0.017(1)	O31	4	0.8834(5)	0.9454(5)	0.5207(6)	1	0.033(2)
T14	4	0.6924(2)	0.9728(2)	0.4387(2)	1 [0.95(1)][d]	0.020(1)	O32	4	0.7586(5)	0.9480(5)	0.4971(7)	1	0.042(2)
T15	4	0.7203(2)	0.9394(2)	0.2196(2)	1 [0.96(1)][d]	0.016(1)	O33	4	0.6257(5)	0.1547(5)	0.4859(6)	1	0.030(2)
T16	4	0.8778(2)	0.9371(2)	0.2226(2)	1 [0.95(1)][d]	0.016(1)	O34	4	0.6919(6)	0.1577(5)	0.3229(7)	1	0.042(2)
T17	4	0.9281(2)	0.9727(1)	0.4363(2)	1 [0.96(1)][d]	0.014(1)	O35	4	0.8007(5)	0.1561(5)	0.2271(6)	1	0.041(2)
T18	4	0.8130(2)	0.9400(2)	0.5781(2)	1 [0.94(1)][d]	0.019(1)	O36	4	0.9045(4)	0.1670(5)	0.3360(6)	1	0.043(2)
T19	4	0.5770(2)	0.1724(2)	0.5767(2)	1 [0.98(1)][d]	0.014(1)	O37	4	0.8846(4)	0.1512(4)	0.5276(6)	1	0.034(2)
T20	4	0.6917(2)	0.1293(2)	0.4357(2)	1 [0.98(1)][d]	0.016(1)	O38	4	0.7533(6)	0.1647(6)	0.4879(7)	1	0.048(2)
T21	4	0.7255(2)	0.1735(2)	0.2208(2)	1 [0.94(1)][d]	0.022(1)	O39	4	0.6863(6)	0.0530(5)	0.4433(8)	1	0.069(3)
T22	4	0.8784(2)	0.1739(2)	0.2217(2)	1 [0.94(1)][d]	0.016(1)	O40	4	0.9215(5)	0.0518(5)	0.4219(6)	1	0.035(2)
T23	4	0.9288(1)	0.1307(2)	0.4322(2)	1 [0.96(1)][d]	0.015(1)	O41	4	0.5820(4)	0.8704(4)	0.6380(6)	1	0.041(2)
T24	4	0.8129(2)	0.1726(2)	0.5702(2)	1 [0.94(1)][d]	0.018(1)	O42	4	0.5946(5)	0.0003(4)	0.6627(6)	1	0.031(2)
O1	4	0.3742(5)	0.0477(5)	0.0100(7)	1	0.048(3)	O44	4	0.8098(4)	0.8708(4)	0.6319(5)	1	0.028(2)
O2	4	0.3095(5)	0.0517(5)	0.1674(6)	1	0.046(2)	O45	4	0.8089(5)	0.9971(5)	0.6593(6)	1	0.038(2)
O3	4	0.2016(5)	0.0604(5)	0.2829(6)	1	0.054(2)	O46	4	0.8072(5)	0.1301(5)	0.6689(6)	1	0.037(2)
O4	4	0.0986(4)	0.0625(5)	0.1631(5)	1	0.032(2)	O47	4	0.0028(4)	0.9479(4)	0.4580(6)	1	0.023(2)
O5	4	0.1139(4)	0.0529(5)	0.9703(6)	1	0.027(2)	O48	4	0.0049(4)	0.1531(4)	0.4562(6)	1	0.029(2)
O6	4	0.2470(5)	0.0587(5)	0.0053(7)	1	0.040(2)	Li1	4	0.076(2)	0.738(5)	0.053(5)	0.6(1)	0.08
O7	4	0.3742(6)	0.8405(6)	0.0127(8)	1	0.053(3)	Li2	4	0.817(4)	0.088(3)	0.462(6)	0.5(1)	0.08
O8	4	0.3081(5)	0.8468(4)	0.1739(6)	1	0.036(2)	Li3	4	0.470(3)	0.097(3)	0.763(3)	0.4(1)	0.08
O9	4	0.1979(5)	0.8458(4)	0.2829(6)	1	0.040(2)	Li4	4	0.310(5)	0.728(4)	0.049(7)	0.3(1)	0.08
O10	4	0.0876(5)	0.8437(5)	0.1789(6)	1	0.043(2)	N1	4	1.000(2)	0.133(2)	0.788(2)	0.3(1)	0.05
O11	4	0.1188(5)	0.8394(5)	0.9887(7)	1	0.043(2)	N2	4	0.989(1)	0.811(1)	0.689(1)	0.5(1)	0.05
O12	4	0.2435(6)	0.8466(5)	0.0031(7)	1	0.047(3)	C1	4	0.576(1)	0.237(1)	0.892(1)	0.5(1)	0.05
O13	4	0.3003(5)	0.9490(5)	0.0704(7)	1	0.058(3)	C2	4	0.052(1)	0.243(2)	0.010(2)	0.3(1)	0.05
O14	4	0.0760(5)	0.9486(5)	0.0692(7)	1	0.047(2)	C3	4	0.981(1)	0.247(2)	0.864(1)	0.6(1)	0.05
O15	4	0.4164(5)	0.1241(6)	0.8563(7)	1	0.057(3)	C4	4	0.001(1)	0.844(1)	0.774(2)	0.5(1)	0.05
O16	4	0.4091(6)	0.9984(5)	0.8375(7)	1	0.041(2)	C5	4	0.030(1)	0.089(1)	0.715(3)	0.5(1)	0.05
O17	4	0.3997(5)	0.8678(5)	0.8283(6)	1	0.038(2)	C6	4	1.000(1)	0.909(1)	0.796(1)	0.6(1)	0.05
O18	4	0.1874(4)	0.1296(4)	0.8601(6)	1	0.036(2)	C7	4	0.208(2)	0.736(2)	0.551(2)	0.3(1)	0.05

[a] The final R1 value converged to 0.08 ($R1 = \sum||F_o| - |F_c||/\sum|F_o|$) for 5537 reflections [$|F_o| > 4\sigma(|F_o|)$] in space group $P2_12_12_1$. Refined lattice parameters: $a = 19.793(4)$ Å; $b = 19.766(4)$ Å; $c = 13.266(3)$ Å. [b] M, multiplicity. [c] U_{Iso}, isotropic displacement. [d] Occupancies of silicon atoms were obtained while their displacement parameters on T sites were fixed to 0.015, a typical U_{iso} value for T sites in the MFI.[14] All T sites are randomly occupied by silicon and lithium cations over the framework.

Direct methods revealed the framework associated with MFI. After locating the 24 symmetrically independent T-sites and 48 O-sites positional and displacement parameters for these sites were refined. We imposed no constraint on the framework geometry during these refinements. Several peaks in Fourier difference maps calculated on the basis of these refined models suggested the location of possible extraframework sites for lithium, and for nitrogen and carbon associated with the tetrapropylammonium (TPA) cations. Assignments were based upon expected interatomic distances and the geometry expected for the TPA. Four nitrogen, eight nonframework Li^+ cations, and several sites partially occupied by carbon were determined on this basis.

Subsequent refinements then tested the possibility of ordering of Li over the 24 available framework T-sites. Displacement parameters were fixed at reasonable values determined from a precise single-crystal structure determination for the MFI framework[14] in space group $P2_12_12_1$. The scattering factor for silicon was assumed for the species occupying the T-sites and the occupancies of these sites were refined. As would be expected for random Li-substitution, the occupancy factors for all T sites were less than one, with a suggested Si/Li ratio in these sites of 92:4. There is no evidence for significant Li ordering in the framework, such as a significant deviation from the expected average T−O distances; these distances for all sites are about the same, and these would be different if Li orders in some sites (ionic radii are 0.40 Å for Si and 0.59 Å for Li for the four-fold coordination). However, the results are not definitive, as occupancies and displacement parameters are highly correlated, and the scale factor in these refinements effectively becomes determined by the presumption of full occupancy for the framework oxygen sites. The occupancy parameters for the sites partially occupied by carbon were allowed to vary without any restraints during the final cycles of structural refinement with the synchrotron X-ray diffraction data. The refined atomic parameters of the unit cell and bond distances and angles between framework constituents are summarized in Table 1 and Table 2, respectively.

Results and Discussion

Chemical Analysis. Chemical analysis gave a ratio of elements for as-synthesized [Li−Si−O]-MFI of Si/Li/TPA = 7.6:1:0.3−0.4. This result in itself is indicative of Li substitution into the framework, because the presence of a significant number of charge-balancing cations strongly suggests that framework substitution has occurred. Considering Si and Li are the only species (apart from H^+) present in the synthesis gel that are capable of incorporation into the framework, this suggests that Li^+ is substituting for Si^{4+} in the framework.

Table 2. Interatomic Bond Lengths *d*(T−O) [Å] and Angles ∠(OTO) [°] in the Framework Structure of As-Synthesized [Li−Si−O]-MFI[a]

	d(T−O) [Å]		∠(OTO) [°]		*d*(T−O) [Å]		∠(OTO) [°]
T1−O15	1.53 (1)	O15−T1−O16	108.0 (1)	T13−O27	1.53 (1)	O27−T13−O21	110.6 (1)
T1−O16	1.56 (1)	O15−T1−O47	108.4 (1)	T13−O21	1.55 (1)	O27−T13−O42	113.3 (1)
T1−O47	1.59 (1)	O15−T1−O1	116.5 (1)	T13−O42	1.58 (1)	O27−T13−O41	105.6 (1)
T1−O1	1.61 (1)	O16−T1−O47	110.6 (1)	T13−O41	1.60 (1)	O21−T13−O42	109.2 (1)
		O16−T1−O1	108.8 (1)			O21−T13−O41	108.2 (1)
		O47−T1−O1	104.5 (1)			O42−T13−O41	109.7 (1)
T2−O2	1.50 (1)	O2−T2−O1	108.1 (1)	T14−O32	1.59 (1)	O32−T14−O39	110.4 (1)
T2−O1	1.52 (1)	O2−T2−O6	110.6 (1)	T14−O39	1.60 (1)	O32−T14−O28	108.4 (1)
T2−O6	1.53 (1)	O2−T2−O13	102.9 (1)	T14−O28	1.61 (1)	O32−T14−O27	107.6 (1)
T2−O13	1.58 (1)	O1−T2−O6	112.1 (1)	T14−O27	1.64 (1)	O39−T14−O28	116.5 (1)
		O1−T2−O13	111.4 (1)			O39−T14−O27	108.4 (1)
		O6−T3−O13	111.3 (1)			O28−T14−O27	105.1 (1)
T3−O3	1.53 (1)	O3−T3−O20	107.9 (1)	T15−O28	1.54 (1)	O28−T15−O29	109.8 (1)
T3−O20	1.55 (1)	O3−T3−O19	109.1 (1)	T15−O29	1.57 (1)	O28−T15−O45	109.9 (1)
T3−O19	1.57 (1)	O3−T3−O2	111.8 (1)	T15−O45	1.60 (1)	O28−T15−O46	105.4 (1)
T3−O2	1.65 (1)	O20−T3−O19	107.9 (1)	T15−O46	1.62 (1)	O29−T15−O45	109.5 (1)
		O20−T3−O2	112.5 (1)			O29−T15−O46	112.4 (1)
		O19−T3−O2	107.5 (1)			O45−T15−O46	109.7 (1)
T4−O3	1.57 (1)	O3−T4−O17	106.3 (1)	T16	1.55 (1)	O30−T16−O29	111.2 (1)
T4−O17	1.57 (1)	O3−T4−O16	110.6 (1)	T16	1.55 (1)	O30−T16−O42	108.9 (1)
T4−O16	1.59 (1)	O3−T4−O4	109.6 (1)	T16	1.57 (1)	O30−T16−O43	105.4 (1)
T4−O4	1.59 (1)	O17−T4−O16	110.1 (1)	T16	1.57 (1)	O29−T16−O42	106.4 (1)
		O17−T4−O4	108.9 (1)			O29−T16−O43	113.3 (1)
		O16−T4−O4	111.2 (1)			O42−T16−O43	111.7 (1)
T5−O4	1.55 (1)	O4−T5−O21	111.7 (1)	T17−O31	1.53 (1)	O31−T17−O40	113.0 (1)
T5−O21	1.56 (1)	O4−T5−O14	113.9 (1)	T17−O40	1.58 (1)	O31−T17−O47	107.4 (1)
T5−O14	1.57 (1)	O4−T5−O5	109.5 (1)	T17−O47	1.59 (1)	O31−T17−O30	109.5 (1)
T5−O5	1.61 (1)	O21−T5−O14	108.0 (1)	T17−O30	1.60 (1)	O40−T17−O47	113.9 (1)
		O21−T5−O5	106.4 (1)			O40−T17−O30	106.2 (1)
		O14−T5−O5	107.0 (1)			O47−T17−O30	106.7 (1)
T6−O5	1.57 (1)	O5−T6−O19	106.8 (1)	T18−O32	1.53 (1)	O32−T18−O44	112.9 (1)
T6−O19	1.57 (1)	O5−T6−O6	113.9 (1)	T18−O44	1.54 (1)	O32−T18−O45	111.9 (1)
T6−O6	1.62 (1)	O5−T6−O18	106.4 (1)	T18−O45	1.56 (1)	O32−T18−O31	105.9 (1)
T6−O18	1.62 (1)	O19−T6−O6	110.5 (1)	T18−O31	1.59 (1)	O44−T18−O45	108.6 (1)
		O19−T6−O18	109.1 (2)			O44−T18−O31	108.4 (1)
		O6−T6−O18	110.0 (1)			O45−T18−O31	109.1 (1)
T7−O48	1.54 (1)	O48−T7−O7	108.4 (1)	T19−O23	1.57 (1)	O23−T19−O33	111.6 (1)
T7−O7	1.55 (1)	O48−T7−O23	108.9 (1)	T19−O33	1.58 (1)	O23−T19−O22	109.8 (1)
T7−O23	1.56 (1)	O48−T7−O17	111.8 (1)	T19−O22	1.58 (1)	O23−T19−O43	108.2 (1)
T7−O17	1.57 (1)	O7−T7−O23	108.5 (1)	T19−O43	1.60 (1)	O33−T19−O22	106.8 (1)
		O7−T7−O17	110.2 (1)			O33−T19−O43	112.3 (1)
		O23−T7−O17	108.9 (1)			O22−T19−O43	108.0 (1)
T8−O8	1.53 (1)	O8−T8−O12	114.7 (1)	T20−O39	1.52 (1)	O39−T20−O33	103.5 (1)
T8−O12	1.56 (1)	O8−T8−O13	103.5 (1)	T20−O33	1.55 (1)	O39−T20−O38	118.1 (1)
T8−O13	1.58 (1)	O8−T8−O7	106.7 (1)	T20−O38	1.57 (1)	O39−T20−O34	114.3 (1)
T8−O7	1.59 (1)	O12−T8−O13	104.5 (1)	T20−O34	1.60 (1)	O33−T20−O38	108.7 (1)
		O12−T8−O7	110.7 (1)			O33−T20−O34	106.9 (1)
		O13−T8−O7	116.9 (1)			O38−T20−O34	104.8 (1)
T9−O18	1.53 (1)	O18−T9−O25	109.3 (1)	T21−O35	1.53 (1)	O35−T21−O34	109.1 (1)
T9−O25	1.55 (1)	O18−T9−O9	109.1 (1)	T21−O34	1.54 (1)	O35−T21−O25	111.3 (1)
T9−O9	1.59 (1)	O18−T9−O8	106.7 (1)	T21−O25	1.60 (1)	O35−T21−O44	109.7 (1)
T9−O8	1.60 (1)	O25−T9−O9	109.9 (1)	T21−O44	1.63 (1)	O34−T21−O25	109.3 (1)
		O25−T9−O8	111.6 (1)			O34−T21−O44	110.1 (1)
		O9−T9−O8	110.4 (1)			O25−T21−O44	107.3 (1)
T10−O10	1.53 (1)	O10−T10−O15	104.7 (1)	T22−O35	1.58 (1)	O35−T22−O36	104.6 (1)
T10−O15	1.54 (1)	O10−T10−O26	111.4 (1)	T22−O36	1.61 (1)	O35−T22−O41	112.5 (1)
T10−O26	1.56 (1)	O10−T10−O9	112.0 (1)	T22−O41	1.62 (1)	O35−T22−O26	111.9 (1)
T10−O9	1.59 (1)	O15−T10−O26	110.9 (1)	T22−O26	1.65 (1)	O36−T22−O41	116.4 (1)
		O15−T10−O9	107.4 (1)			O36−T22−O26	106.0 (1)
		O26−T10−O9	110.2 (1)			O41−T22−O26	105.4 (1)
T11−O14	1.55 (1)	O14−T11−11	111.7 (1)	T23−O36	1.54 (1)	O36−T23−O40	111.1 (1)
T11−O11	1.56 (1)	O14−T11−O22	109.6 (1)	T23−O40	1.57 (1)	O36−T23−O37	111.6 (1)
T11−O22	1.55 (1)	O14−T11−O10	108.1 (1)	T23−O37	1.59 (1)	O36−T23−O48	109.2 (1)
T11−O10	1.59 (1)	O11−T11−O22	109.1 (1)	T23−O48	1.60 (1)	O40−T23−O37	105.7 (1)
		O11−T11−O10	111.5 (1)			O40−T23−O48	112.2 (1)
		O22−T11−O10	107.8 (1)			O37−T23−O48	106.8 (1)

Table 2 (Continued)

	d(T−O) [Å]		∠(OTO) [°]		*d*(T−O) [Å]		∠(OTO) [°]
T12−O12	1.53 (1)	O12−T12−O24	115.4 (1)	T24−O46	1.56 (1)	O46−T24−O37	102.8 (1)
T12−O24	1.57 (1)	O12−T12−O11	106.1 (1)	T24−O37	1.58 (1)	O46−T24−O24	106.6 (1)
T12−O11	1.58 (1)	O12−T12−O20	106.1 (1)	T24−O24	1.59 (1)	O46−T24−O38	117.5 (1)
T12−O20	1.58 (1)	O24−T12−O11	107.3 (1)	T24−O38	1.62 (1)	O37−T24−O24	110.9 (1)
		O24−T12−O20	107.5 (1)			O37−T24−O38	112.8 (1)
		O11−T12−O20	114.7 (1)			O24−T24−O38	106.1 (1)
Li1−O36	2.07 (1)						
Li1−O37	2.17 (1)						
Li1−O48	2.33 (1)						
Li1−O11	2.34 (1)						
Li2−O38	2.00 (1)						
Li2−O37	2.03 (1)						
Li2−O40	2.26 (1)						
Li3−O15	1.71 (1)						
Li3−O10	1.97 (1)						
Li3−O16	2.50 (1)						
Li4−O38	1.85 (1)						
Li4−O33	1.97 (1)						
Li4−O34	2.20 (1)						
Li4−O37	2.60(1)						

[a] In addition, interatomic boding lengths between extraframework lithiums and framework oxygens are given at the bottom of the table.

Proton (charge balancing) defects may also be present. These will be discussed in more detail later.

Diffraction & Crystallography. The powder X-ray diffraction patterns of as-synthesized [Li−Si−O]-MFI, silicates, and Li−ZSM-5(Al) confirm that each material is free of crystalline impurities, and all have structures characteristic of the orthorhombic MFI structure type (a = 20.022 Å; b = 19.899 Å; c = 13.383 Å).[14] All the peaks in the pattern could be indexed on the basis of this cell. There are, however, distinguishable differences in the relative intensities of each of the materials, which are most clearly seen in the regions $7° < 2\theta < 10°$ and $22.5° < 2\theta < 25°$ (Figure 1). The [Li−Si−O]-MFI framework bonding distances, *d*(T−O), and occupancies on T sites are consistent with complete disordering of Si and Li cations on the available framework T sites (Tables 1 and 2). The substitution of Li in the MFI framework alone would not be expected to result in significant intensity differences, as the net change in scattering power from each T site is small. Rather, these intensity changes are likely indicative of structural differences between [Li−Si−O]-MFI, silicalite, and Li−ZSM-5(Al). We attribute these intensity changes, as well as the reduction in symmetry from *Pnma* to $P2_12_12_1$, to the change in the ratio of TPA^+ to Li^+ in extraframework sites. Nonframework lithium ions are occluded in four different sites within narrow cage-like voids outlined by the double five-membered-rings (5MR) or 6MR (Figure 2). These are either 3-fold or 4-fold coordinated to framework oxygen atoms with a distance range of 1.71(1)−2.60(1) Å (Table 2). This indicates a strong interaction between the extraframework Li^+ cations and the negatively charged framework. For TPA^+ cations there are two different sites inside the 10MR-channels.

The distribution of extraframework lithium cations within the small pore voids may serve to stabilize this new lithosilicate structure. Interestingly, the TPA^+ cation in [Li−Si−O]-MFI is not as readily removed by calcination as the TPA^+ cation in ZSM-5, requiring a temperature of 823 K for 7 days, compared to 823 K for 5 h for ZSM-5. This suggests that TPA^+ may play an important role in charge compensation as well as acting as a structure-directing or template agent during the synthesis of MFI frameworks.

The MFI framework is known to undergo a number of changes in symmetry, as a function of sorbent, temperature, etc.[15] and the assignment of the symmetry change to the presence of the extraframework cations is not definitive. For example, symmetry lowering was recently observed for TPA-ZSM-5 with Si/Al = 23 (i.e., $(TPA^+)_4[Al_4Si_{92}O_{192}]$) by Yokomori and Idaka, who suggested that the change in space group to $Pn2_1a$ is likely due to ordering of the framework Al atoms.[16] The significant overlap of many reflections in the powder diffraction data of [Li−Si−O]-MFI, caused by the large pseudo-tetragonal unit cell, precludes further analysis of the powder diffraction data, and it is difficult to establish whether the similar lowering of symmetry from *Pnma* to $P2_12_12_1$ is due to Li ordering.

NMR Spectroscopy. Additional evidence for the presence of framework lithium cations in [Li−Si−O]-MFI was found in the ^{29}Si MAS NMR spectra. The spectra contain two broad resonances at −101.5 and −113.5 ppm. These are assigned to Q^4(1Li,3Si) and Q^4(0Li,4Si), respectively, based upon comparison with the ^{29}Si MAS NMR of other lithosilicates, which yielded a range of chemical shifts for Q^4(1Li,3Si) environments of between −88 and −100 ppm.[4−6,8] The two resonances can be deconvoluted giving an integrated intensity ratio of Q^4(1Li,3Si) to Q^4(0Li,4Si) of 1:4.6 (Figure 3). The number of framework Li cations per unit cell (x) can be calculated from the formula $I_{Q^4(1Li,3Si)}/I_{Q^4(4Si)} = 4x/(N - 5x)$[17] where N = 96, the total number of T atoms in the unit cell, yielding an estimate for x of 4.1. The Li content determined by NMR may be overestimated due to the presence of defect sites such as SiOH groups in the [Li−Si−O]-MFI framework. In particular, if any Si(1OH3Si) defects are present, these will give to rise resonances

(15) For example, Gies, H.; Marler, B.; Fyfe, C.; Kokotailo, G.; Feng, Y.; Cox, D. E. *J. Phys. Chem. Solids* **1991**, *52* (10), 1235.

(16) Yokomori, Y.; Idaka, S. *Microporous Mesoporous Mater.* **1999**, *28*, 405−413.

(17) Engelhardt, G.; Michel, D. *High-Resolution Solid-State NMR of Silicates and Zeolites*; Wiley: New York, 1987.

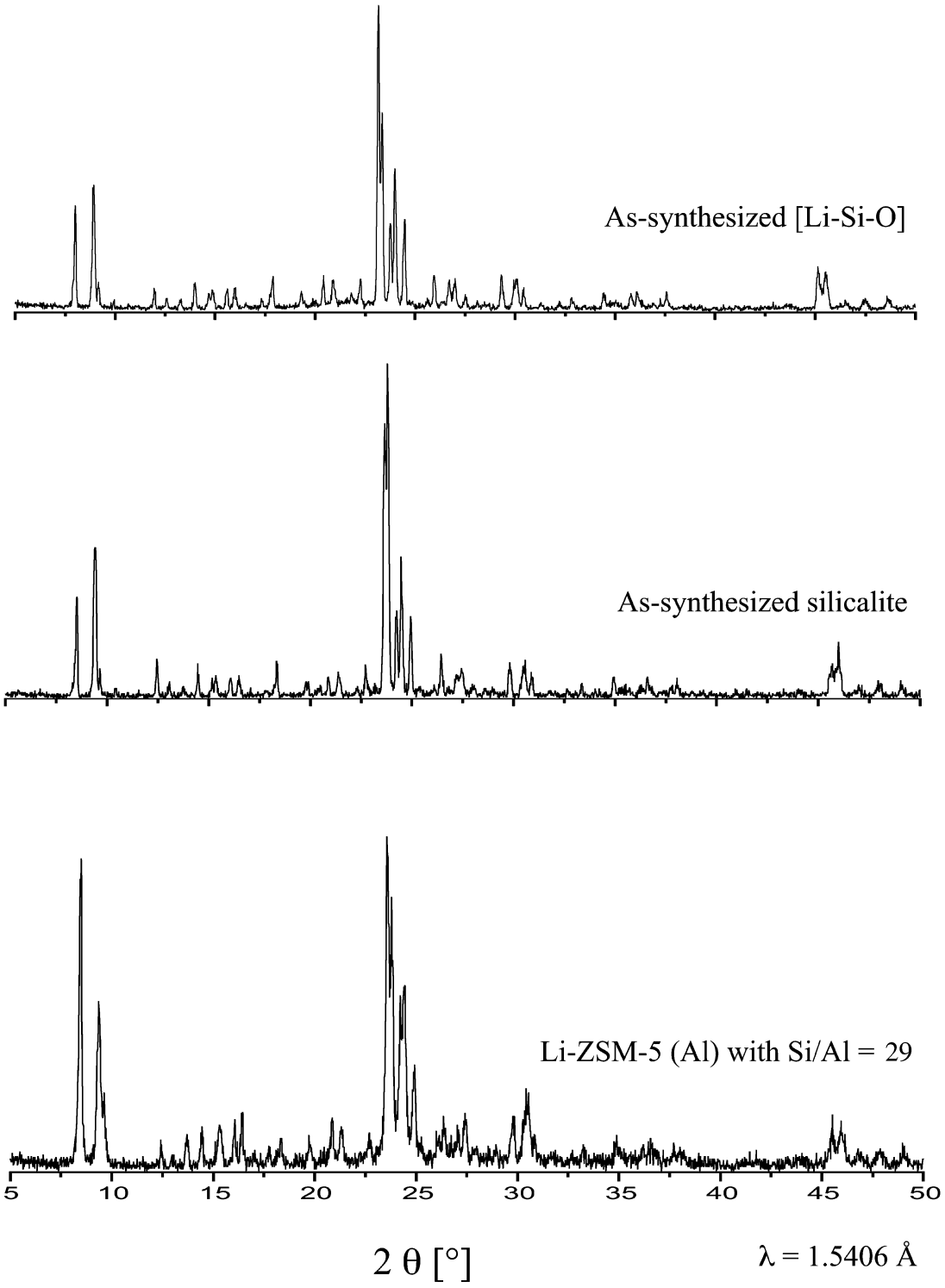

Figure 1. XPD of as-synthesized [Li−Si−O]-MFI (top), silicalite (middle), and Li−ZSM-5(Al) (bottom).

between −97 to −109 ppm that will overlap with the Si(1Li,3Si) resonances.[17,18] However, the chemical analysis, ^{29}Si NMR, and structure determination are all consistent with the idealized formula $TPA^{+}_{4}Li^{+}_{8}[Li_4Si_{92}O_{192}]$ for as-synthesized [Li−Si−O]-MFI.

Variable-temperature (VT) ^{7}Li and ^{1}H MAS NMR experiments on a dehydrated, calcined [Li−Si−O]-MFI sample loaded with 100 Torr of oxygen showed that the extraframework Li cations are inaccessible to oxygen, but that the protons formed on calcination are accessible to gas molecules. Upon lowering the temperature, no change in the ^{7}Li chemical shift was seen (Figure 4), indicating no direct $Li^{+}-O_2$ contacts;[19,20] larger spinning sidebands were observed however, consistent with the sorption of O_2 into the channel systems, and with the

(18) Jacobsen, C. J. H.; Madsen, C.; Janssens, T. V. W.; Jakobsen, H. J.; Skibsted, J. *Microporous Mesoporous Mater.* **2000**, *39*, 393−401.

(19) Accardi, R. J.; Lobo, R. F. *Microporous Mesoporous Mater.* **2000**, *40*, 25−34.

(20) Plevert, J.; Menoral, L. C.; Renzo, F. D.; Fajula, F. *J. Phys. Chem. B* **1998**, *102*, 3412−3416.

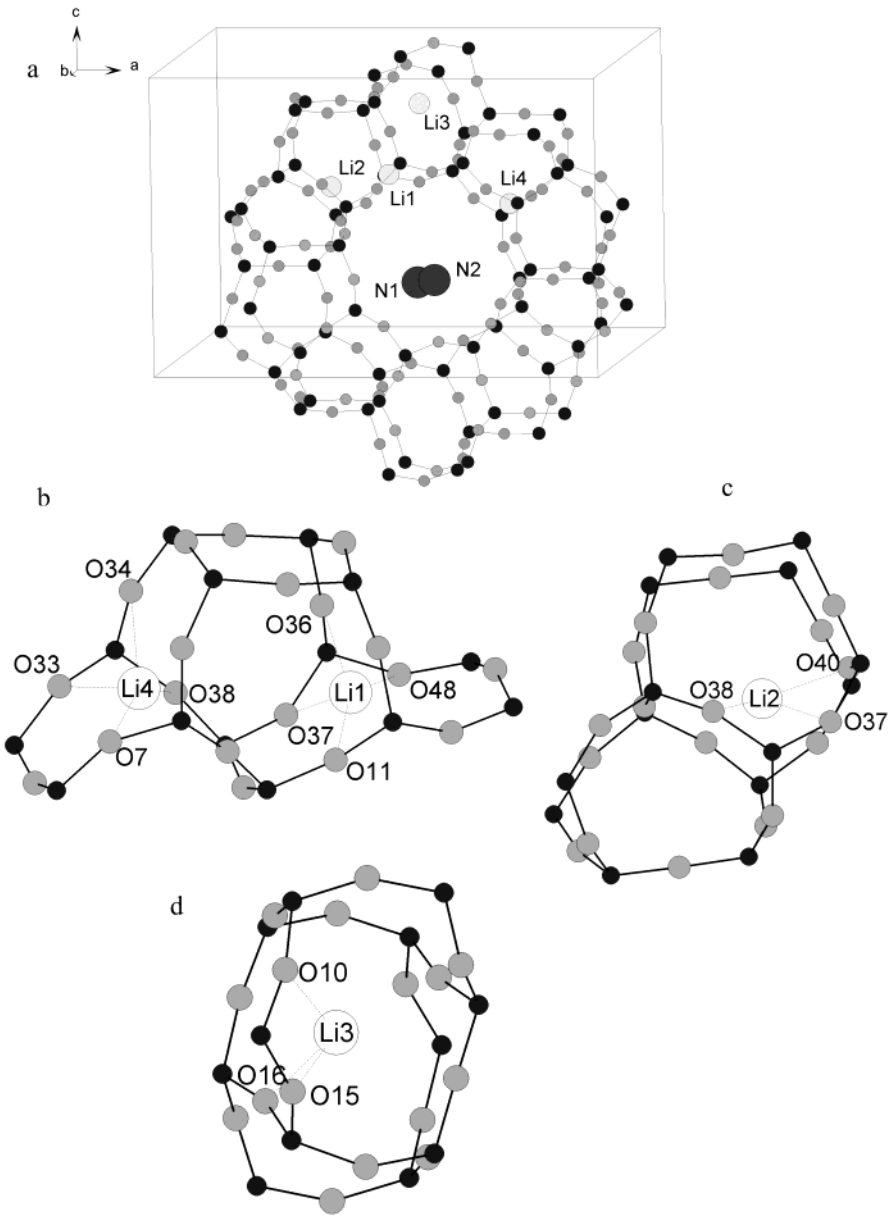

Figure 2. Partial structure of [Li−Si−O]-MFI. (a) ZSM-5 analogue. (b, c, and d) Encapsulated sites available for nonframework Li cations, Li1 (along with Li4), Li2, and Li3, respectively, are enlarged. Lithium and silicon atoms (dark, small circles) are statically disordered to build the framework with oxygen atoms (light gray, small circles). Extraframework lithium cations are occluded in narrow pore voids (medium circles) while the large TPA^+ cations are present in the 10MR-channels (dark, large circles).

location of the lithium ions in the 5 and 6MRs. In contrast, the ^{1}H MAS NMR spectra (Figure 5) showed not only an increase in sideband intensity, but also shifts of the isotropic resonance to lower frequency, similar to the behavior of H−ZSM-5[21], indicating a direct interaction between H^+ and O_2.

Previous studies of zeolites H−ZSM-5(Al) using ^{1}H MAS NMR revealed two major groups of ^{1}H MAS NMR resonances: bridging Si−OH−Al groups (Brønsted acid sites) at 4 and 7 ppm and the nonacidic sites, i.e., silanol (SiOH) groups at around 2 ppm.[22,23] In ^{1}H MAS NMR spectra of O_2-loaded H−ZSM-5, the acidic protons of bridging Si−OH−Al groups were strongly affected by the paramagnetic adsorbed oxygen molecules, whereas the silanol groups were only weakly affected. The Brønsted-acid-site−O_2 interaction increased with decreasing temperature (the resonances shifting only slightly to lower frequency), while the width of the sideband manifolds increased dramatically. The ^{1}H MAS NMR spectra of calcined, dehydrated [Li−Si−O]-MFI contain two resonances at 1 and 3.5 ppm from two different OH groups at room temperature. The intensities of the sidebands of both these MAS NMR resonances increase at lower temperatures, indicating that both OH groups are accessible to O_2. Furthermore, the shift and increase in sideband manifold intensity is much more dramatic than was observed for the Si−OH group in ZSM-5, suggesting that the sites in Li-[MFI] are more acidic.

(21) Liu, H.; Kao, H. M.; Grey, C. P. *J. Phys. Chem. B* **1999**, *103*, 4786−4796.
(22) Freund, D. *Chem. Lett.* **1995**, *235*, 69−75.
(23) Hunger, M.; Ernst, S.; Steuernagel, S.; Weitkamp, J. *Microporous Mesoporous Mater.* **1996**, *6*, 349−353.

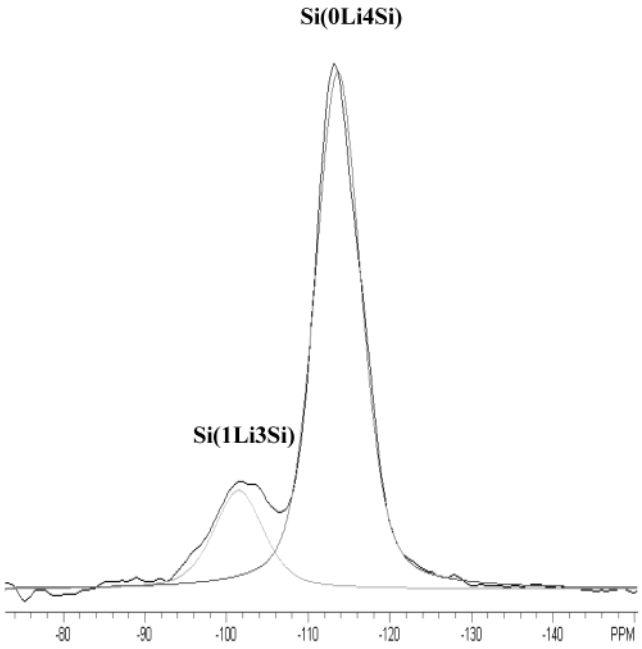

Figure 3. ^{29}Si MAS NMR spectrum of as-synthesized [Li−Si−O]-MFI and its deconvolution into two broad resonance peaks. These are assigned to two different types of framework Si: Si(1Li,3Si) at −101.5 ppm and Si(4Si) at −113.5 ppm. From the ratio of their intensities, the framework Li content was calculated to be 4.1 Li per unit cell, which is consistent with observations from the synchrotron single-crystal diffraction refinement.

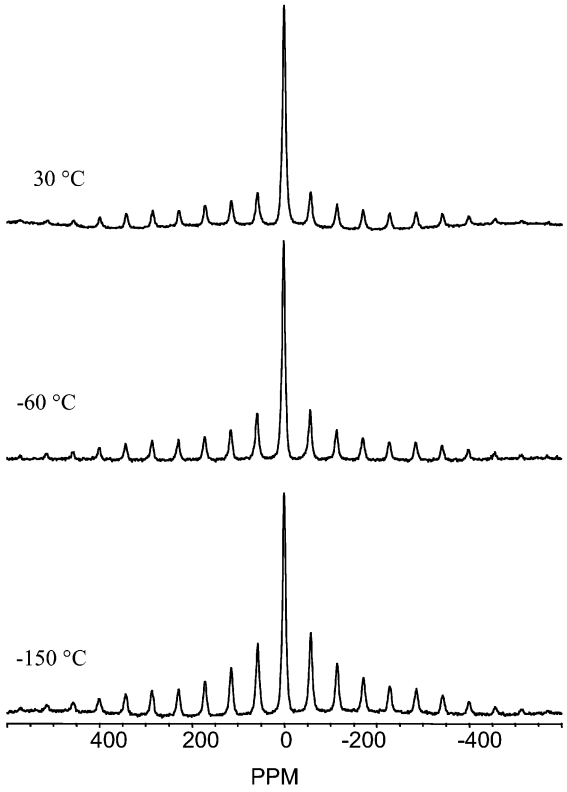

Figure 4. Variable-temperature ^{7}Li MAS NMR spectra of dehydrated, calcined [Li−Si−O]-MFI loaded with 100 Torr of O_2.

Protons in at least one of these OH groups must originate from the charge-compensating TPA^+ group. On dehydration and decomposition of a TPA^+ cation, a proton must still remain, which will be bound to either a Li−O−Si type linkage or a $Si-O^-$ defect present in the framework. The stability of Li−O−Si linkage is not known, but based on observations for boron-substituted zeolites[24] it is likely that the Li−O bond will be broken or considerably weakened on protonation and that a $Li^{+}\cdots O(H)$-Si group will be formed, with the Li^+ ion being only weakly bound to the oxygen of the silanol group. Protonation of a $Si-O^-$ defect will result in a very weak Brønsted acid site, which is not likely to interact strongly with O_2, suggesting that both proton resonances are associated with the framework Li ions. Clearly, a more systematic investigation using ^{1}H MAS NMR for several of the newly developed microporous lithosilicate materials is required to determine the chemical shift parameters for Si−O(H)−Li linkages and Si−OH groups in this system, to relate shift to local structure, and to identify any differences that exist between these groups and the defects in nonlithiated high-silica molecular sieves.

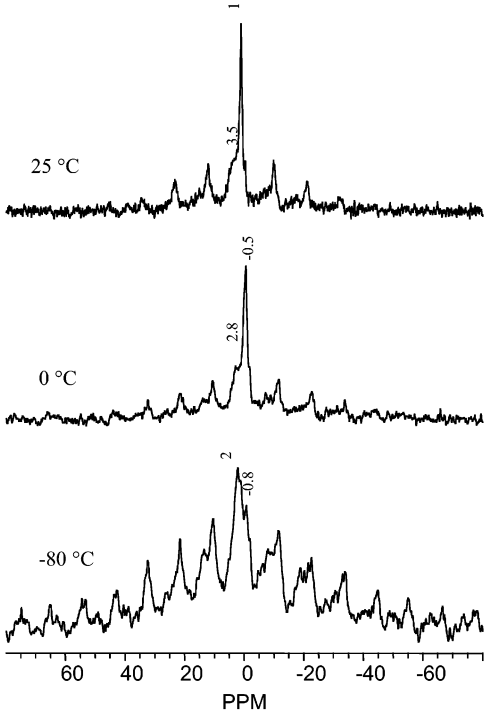

Figure 5. Variable-temperature ^{1}H MAS NMR spectra of dehydrated, calcined [Li−Si−O]-MFI loaded with 100 Torr of O_2.

IR Spectroscopy. Infrared spectra of as-synthesized and calcined [Li−Si−O]-MFI samples are also consistent with the presence of Li−O−Si moieties within the structure. Two IR bands at 863 and 740 cm^{-1} were clearly resolved in the case of as-synthesized [Li−Si−O]-MFI, whereas these bands are absent in the IR spectra of silicalite, as well as those of Li−ZSM-5 (Al) (Figure 6). Even after calcination, the positions of these IR bands of [Li−Si−O]-MFI shift only slightly to 854 and 733 cm^{-1} (Figure 7). Consequently, the presence of the IR peaks at ∼850−860 cm^{-1} and ∼730−740 cm^{-1} for the [Li−Si−O]-MFI material (Figure 6), as well as for several other lithosilicates with well-defined crystal

(24) Fild, C.; Shantz, D. F.; Lobo, R. F.; Koller, H. *Phys. Chem. Chem. Phys.* **2000**, *2* (13), 3091−3098.

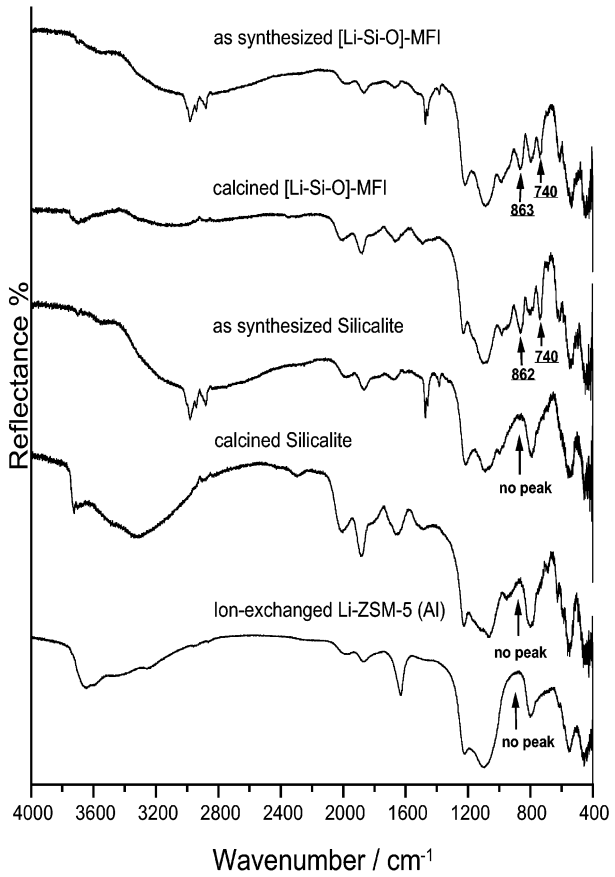

Figure 6. IR spectra of various MFI-related materials. From top to bottom: (a) as-synthesized [Li−Si−O]-MFI, (b) calcined [Li−Si−O]-MFI, (c) as-synthesized silicalite, (d) calcined silicalite, (e) and Li−ZSM-5. The extra IR band at 862−863 and 740 cm^{-1} was observed exclusively in [Li−Si−O]-MFI and, hence, can be ascribed to the incorporation of Li into the framework.

structures (β-eucryptite (β-$LiAlSiO_4$) and lithium metasilicate (Li_2SiO_3), for example), appear to be IR fingerprint bands indicative of a Li−O−Si connection within lithosilicate frameworks.[25,26] We tentatively assign these bands to a Li−O−Si symmetric stretching vibration, on the basis of an analogy to zincosilicates. Only a very weak peak is seen in the as-synthesized [Li−Si−O]-MFI sample at ∼3750 cm^{-1} in the OH stretch region, supporting the assignment of the ^{29}Si NMR resonance at −101 ppm to Si(Li,3Si) and not to Si(OH,3Si).

The IR spectra of the other structures incorporating various kinds of T cations such as Zn, Al, B, Ga, Mn, and Ti into their [(T, Si)O_4]-frameworks also possess other characteristic IR bands around 950 cm^{-1} that are attributed to T−O−Si lattice vibrations.[27−31] However, zincosilicate mordenite ([Zn]-M) also exhibited IR bands shifted to lower wavenumbers.[27] Bands at 802 and 705 cm^{-1} in [Zn]-M are assigned to the symmetric stretching vibration of Zn−O−Si. Note that tetrahedrally coordinated Zn^{2+} and Li^+ cations are similar to each other in terms of their ion radii and bonding distances to framework oxygen anions.[32] According to a correlation between the wavenumbers of the stretching T−O−Si vibration bands and the weight of T cations,[33] the symmetric stretching vibration Li−O−Si is expected to be shifted to the higher wavenumber region with respect to those at 802 and 705 cm^{-1} of [Zn]-M. The assignment of new bands at 863 and 740 cm^{-1} in the IR spectra of [Li−Si−O]-MFI to the symmetric stretching vibration Li−O−Si is consistent with these observations.

Conclusions

We conclude that there are both framework and extraframework Li cations in [Li−Si−O]-MFI, based on chemical composition, NMR, IR, and crystallographic evidence, as well as the significant differences between the IR spectra of Li-exchanged ZSM-5 and [Li−Si−O]-MFI. We see no other way to explain the previously presented results. We expect that the insights obtained thus far from the MFI system will be applicable to a wide range of high-silica zeolites.

To facilitate applications of [Li−Si−O]-MFI, the locations of nonframework cations still need to be optimized and the acidity of the Li−O(H)-Si Brønsted acid site needs to be investigated. Specifically, the interaction of adsorbed gas with the extraframework cations or protons in the 10MR-channels is generally considered a prerequisite for applications involving gas sorption, separation, and catalysis.

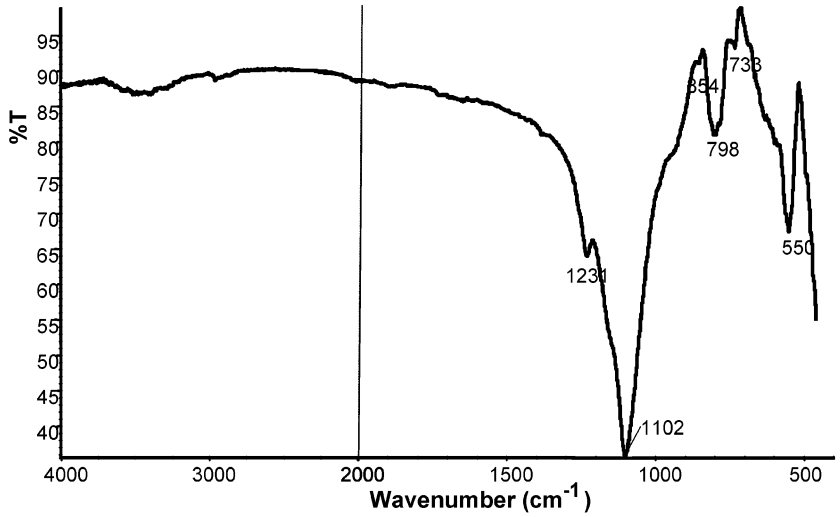

Figure 7. IR spectrum of a dehydrated and calcined sample of [Li−Si−O]-MFI. The fingerprint IR bands for Li−O−Si lattice vibrations are also observed at 854 and 733 cm^{-1} even after water molecules are removed from the microporous material. The bar marked at 2000 cm^{-1} is to show the change in the scale of wavenumber above and below 2000 cm^{-1}.

Acknowledgment. We acknowledge financial support from the NSF and the DOE via CHE-0221934 (CEMS) DMR-0095633 (JBP), and DEFG0296ER14681 (CPG). We are grateful to the NSF and DOE also for their support of the GSECARS facilities at APS. Certain trade names and company products are identified to adequately specify experimental procedures. Such identification does not imply recommendation or endorsement by the National Institute of Standards and Technology, nor does it imply that the products are necessarily the best available for the purpose.

CM049861N

(25) Park, S.-H.; Kleinsorge, M.; Grey, C. P.; Parise, J. B. In *Zeolites and Mesoporous Materials at the Dawn of the 21st Century: Proceedings of the 13th International Zeolite Conference*; Studies in Surface and Catalysis, vol. 135; Galarneau, A., Di Renzo, F., Fajula, F., Vedrine, J., Eds.; Elsevier Science: New York, 2001.

(26) Park, S.-H.; Kleinsorge, M.; Wassmuth, B.; Parise, J. B., submitted for publication.

(27) Dong, M.; Wang, J.; Sun, Y. *Microporous Mesoporous Mater.* **2001**, *43*, 237−243.

(28) Kosslick, H.; Lischke, G.; Walther, G.; Storek, W.; Martin, A.; Fricke, R. *Microporous Mater.* **1997**, *9*, 13−33.

(29) Unneberg, E.; Kolboe, S. *Appl. Catal. A: Gen.* **1995**, *124*, 345−353.

(30) Kim, S. H.; Kim, S. D.; Kim, Y. C.; Kim, C.-S.; Hong, S. B. *Microporous Mesoporous Mater.* **2001**, *42*, 121−129.

(31) Ko, Y. H.; Kim, S. J.; Kim, M. H.; Park, J. H.; Parise, J. B.; Uh, Y. S. *Microporous Mesoporous Mater.* **1999**, *30*, 213−218.

(32) Shannon, R. D. *Acta Crystallogr.* **1976**, *A32*, 759.

(33) Szostack, R. *Molecular Sieves: Principles of Synthesis and Identification*; Van Nostrand Reinhold: New York, 1989, and references therein.